L x rays from low-energy (~2-keV/u) ions with L-shell vacancies produced in single collisions with atoms and molecules

H. Tawara,[1,2] P. Richard,[1] U. I. Safronova,[3] A. A. Vasilyev,[3] S. Hansen,[4] and A. S. Shlyaptseva[4]

[1]*J. R. Macdonald Laboratory, Department of Physics, Kansas State University, Manhattan, Kansas 66506-2601*

[2]*Atomic Physics Division, National Institute of Standards and Technology, Gaithersburg, Maryland 20899-8421*

[3]*Department of Physics, University of Notre Dame, Notre Dame, Indiana 46556-5670*

[4]*Department of Physics, University of Nevada Reno, Reno, Nevada 89557*

(Received 20 July 2001; revised manuscript received 7 January 2002; published 5 April 2002)

Intense L x rays have been observed in ~2-keV/u Kr^{q+} ($q=27$–33) ions colliding with various atom and molecule targets. These x rays are understood to originate from electron capture processes into high-Rydberg states of the projectile ion from the outermost shell of target where the captured electron cascades down into the vacant L shell of the ion, thus emitting L x rays. It has been found that the observed L x-ray spectra move toward higher energy as the ion charge (q) increases. The observed L x-ray spectra are compared with synthetic spectra using various models. It has been found that the L x-ray production cross sections obtained for Kr^{27+} ions are inversely proportional to the ionization energy of target, similar to those recently observed in K x rays produced from ions with K-shell vacancy, and correspond to roughly 40% of total electron capture cross sections, meanwhile the rest of the electron cascades into the metastable states and thus cannot decay within a viewing region of a Si(Li) x-ray detector.

DOI: 10.1103/PhysRevA.65.042509 PACS number(s): 32.30.Rj, 32.70.Cs, 32.80.Rm, 34.70.+e

I. INTRODUCTION

So far a number of experimental and theoretical investigations have been reported for electron-capture processes involving low-energy (~keV/u), highly charged ions colliding with neutral atoms and a reasonable understanding of these electron-capture processes has been obtained [1]. It is known that in such low-energy electron-capture processes an electron is captured into a highly excited Rydberg state of the projectile ion through formation of quasi-molecular ion and the cross sections do not change very much with the collision energy and are roughly constant. On the other hand, if the projectile ion has vacancies in K or L shells, these innershell vacancies can be filled with the captured electron, either directly from the captured Rydberg state or indirectly through a series of cascading-down processes, resulting in K or L x-ray emission. Very recently such x-ray emission processes have been hot topics in astrophysics since the first x rays had been observed in the tail of comets such as Hyakutake [2]. K x-ray emission processes involving ions with a single K-shell vacancy have been recently investigated in some detail and compared with the electron-capture processes [3]. K x rays from bare ions also have been observed [4,5].

In the past, a series of x-ray spectra from heavy, highly charged ions had often been investigated through high-power laser irradiation [6]. Yet the atomic structure parameters are known to be strongly influenced with the presence of the surrounding high-density plasmas [7] and also often the ions emitting x rays are accompanied with some outer-shell electrons which may result in satellite peaks and, thus, x-ray spectrum analysis usually becomes quite complicated.

In the present paper we experimentally study x-ray emission processes from ions with L-shell vacancies which capture an electron from a neutral target under single collisions with a minor contribution of multiple electron capture.

In such electron processes an electron captured into a highly excited ($n_0 l_0$) state of the incident ion gets stabilized after emitting photons or x rays with various energies. The principal quantum number of the most dominant states n_m into which the electron is captured of bare ions with charge q can be estimated through the following relationship [8]:

$$n_m = \frac{q^{0.75}}{(I_b/13.6)^{0.5}}, \tag{1.1}$$

where I_b represents the ionization energy of target species in units of eV. For example, n_m is varied over 9 to 13 for ion-target combinations used in the present studies. Unfortunately there is no simple way of estimating the l_m distributions so far, though a model recently has been proposed but untested yet [9].

The electron captured into such a high-Rydberg state [the following process (1.2)] of ion with L-shell vacancies tends to cascade down through passage of a series of lower intermediate ($n_i l_i$) states via multiple steps [process (1.3)], instead of decaying directly to the ground state via a single step [process (1.4)], before finally reaching the ($2l$) states which, in turn, emit L x rays and then get stabilized

$$A^{q+} + B \rightarrow A^{(q-1)+*}(n_0 l_0) + B^{+} \tag{1.2}$$

$$\rightarrow A^{(q-1)+*}(n'l') \rightarrow A^{(q-1)+*}(n''l'') \rightarrow \cdots \rightarrow A^{(q-1)+}(2l) \tag{1.3}$$

$$\rightarrow A^{(q-1)+}(2l). \tag{1.4}$$

Here (*) indicates the excited state formed after electron capture and cascade. Though the general trend indicates that,

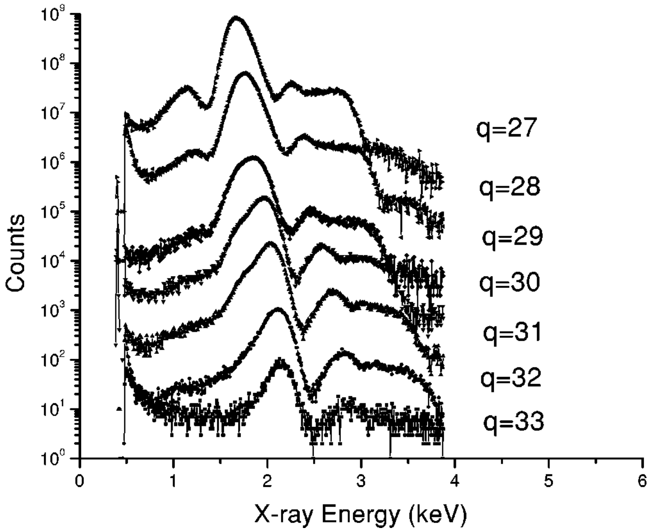

FIG. 1. Typical L x-ray spectra from $\sim$2-keV/uKr^{q+} ($q=27$–33) ions in collisions with Ar atoms, except for Kr^{33+} where target gas was Ne.

as the collision energy increases, n_0 tends to become smaller, meanwhile its distribution becomes broader, such a variation is expected to be relatively small over the present collision energies [1].

It is generally understood that one-electron capture is the most dominant at low-energy, highly charged ion collisions and thus radiative cascade transitions can be important for most of x-ray emission. In some multielectron targets, there are relatively high probabilities where two (or more) electrons are simultaneously captured into nearly the same ($n_0 l_0$) states of projectile ion, thus tending to form autoionization states where one of the captured electrons goes to the continuum, meanwhile the other electron cascades down through the intermediate ($n_i l_i$) states [10] and, then, follows the same process as the single electron-capture process anyway, finally emitting x rays. If these two electrons are captured into significantly different ($n_0 l_0$) states, such states formed tend to follow radiative transitions.

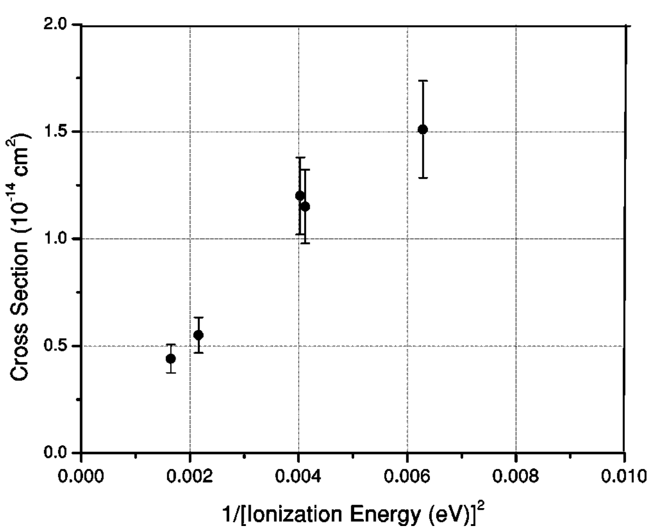

FIG. 2. Total L x-ray production cross sections from Kr^{27+} ions in collisions with various atoms and molecules plotted against the inverse square of the first ionization energy of targets. The error bars represent relative uncertainties.

TABLE I. The observed total L x-ray production cross sections from Kr^{27+} ions colliding with various neutral target atoms and molecules and their ratios to total electron-capture cross sections estimated from an empirical formula [13].

Target	Ionization energy	Cross section	Ratio
	(eV)	(10^{-14}cm^2)	
He	24.59	0.44	0.38
Ne	21.56	0.60	0.37
Ar	15.76	1.20	0.42
N_2	15.58	1.15	0.40
CH_4	12.61	1.51	0.34

II. EXPERIMENTS

The enriched ^{86}Kr^{q+} ($q=27$–33) ions used in the present paper have been provided from Kansas State University electron-beam ion source (EBIS) under the pulsed ion extraction mode. As already described in detail [3], after preacceleration at 6 keV and mass-charge analyzing, about 1 pA Kr^{q+} ions are introduced into a target gas chamber whose pressure is monitored with an MKS Baratron. x rays produced under single collisions of these Kr^{q+} ions with various targets are observed with a Si(Li) detector having 0.0125 mm thick Be window. The observed relative L x ray

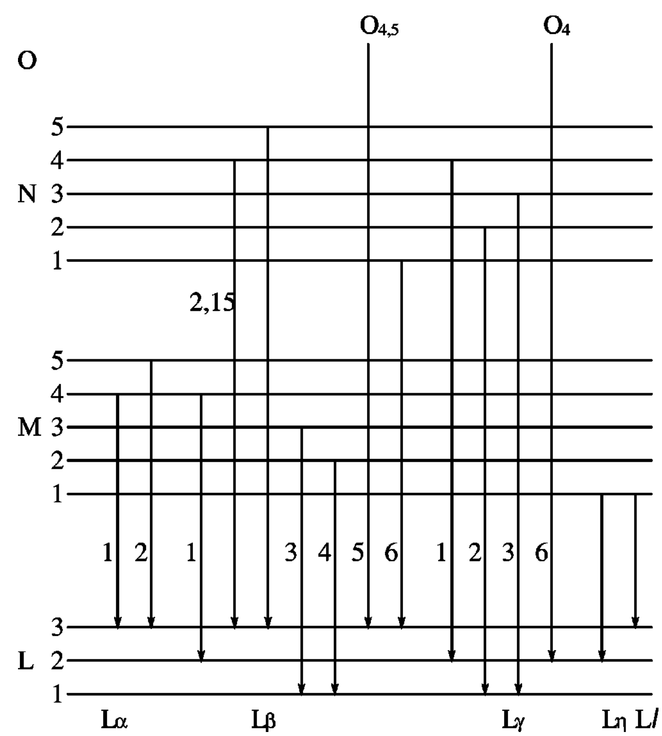

FIG. 3. Transition diagram involving L x-ray emissions. The Siegban notation is used (Ref. [16]). Note that Kr^{27+} ion has a single initial vacancy in the L_3 shell and therefore only limited transitions such as that from M_1 shell are allowed to emit L x rays.

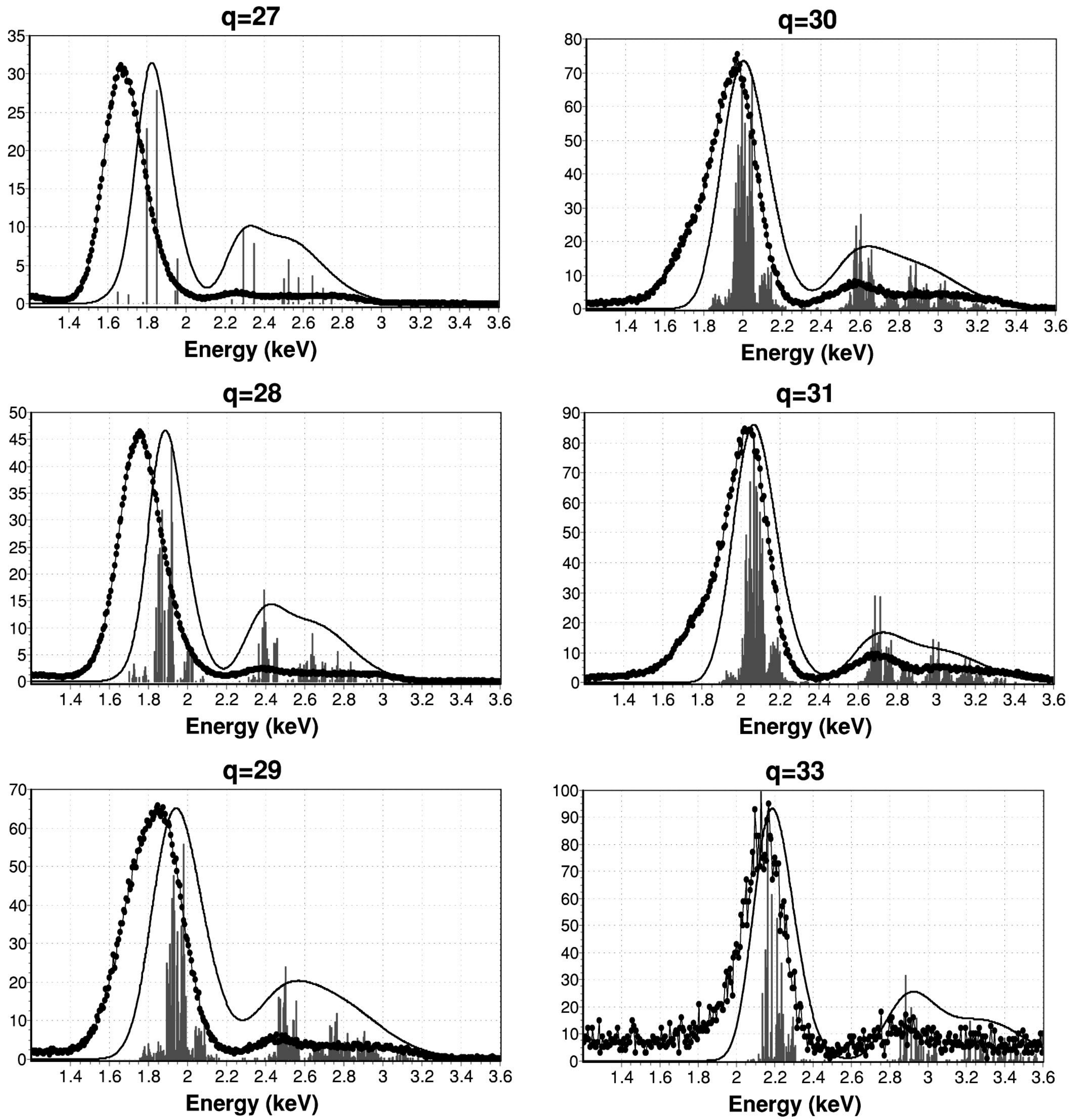

FIG. 4. Comparison between the observed and synthetic *L* x-ray spectra from Kr^{q+} ($q=27$–32) ions colliding with atoms. Only the calculated transition probabilities with statistical populations are used for synthetic spectra.

yields for Kr^{27+} ion impact have been converted into absolute cross sections through normalizing to the known cross sections [11]. Uncertainties in the present cross sections are estimated to be about 25% including those of the normalized cross section. The energy uncertainties in the observed spectra are about 20 eV. Higher charged ($q \geqslant 28$) ions are too weak to be integrated in the present current integrator to get the total number of the incident ions into the target chamber. Therefore, no cross sections can be determined but only *L* x-ray spectra have been observed.

III. RESULTS AND DISCUSSION

A. Observed x-ray spectra for different charge Kr^{q+} ions

General features of typical *L* x-ray spectra observed are shown in Fig. 1 where significant structures are clearly seen. The most intense peaks are found to correspond to *L* x rays,

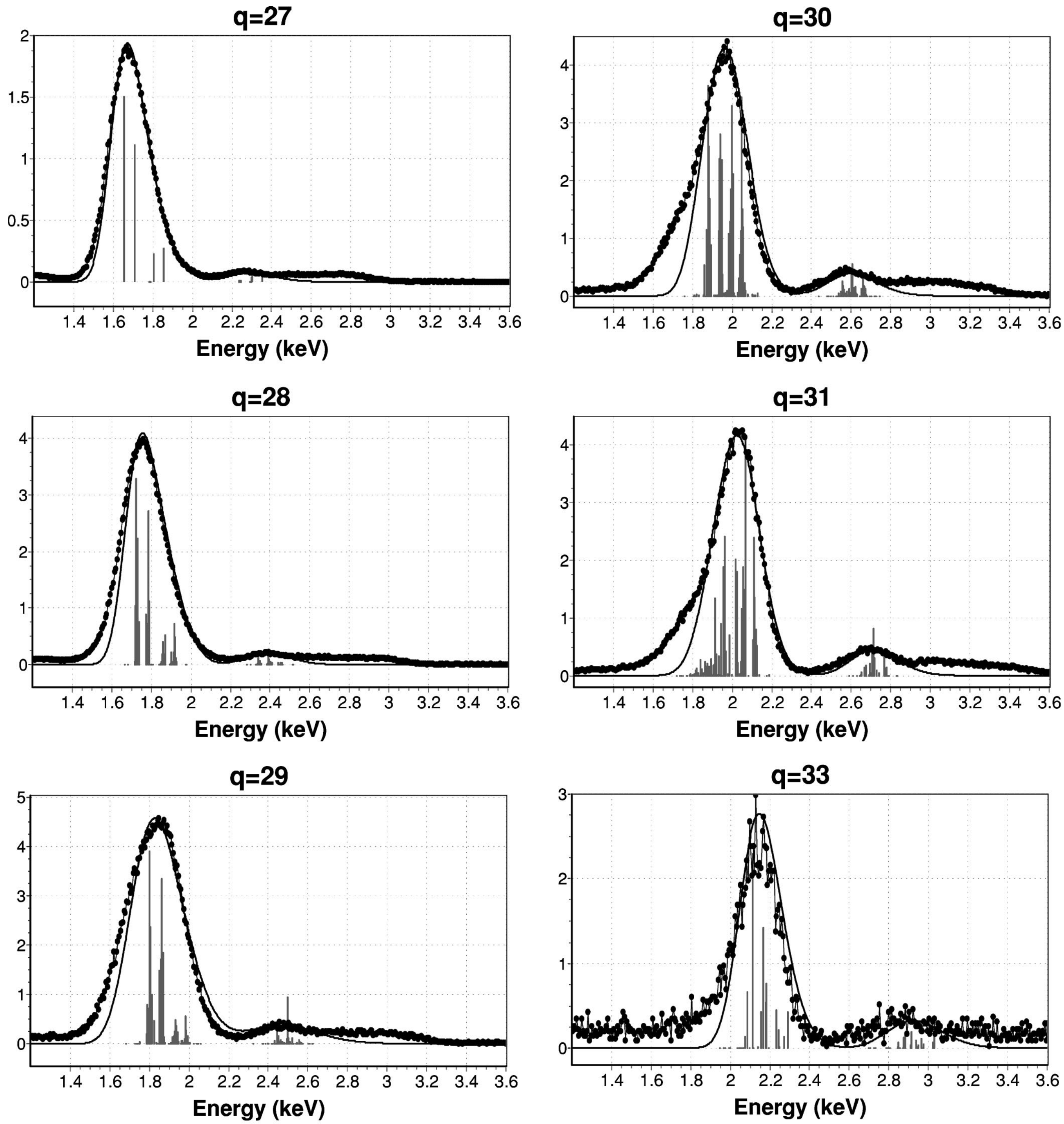

FIG. 5. Comparison between the observed and synthetic L x-ray spectra from Kr^{q+} ($q=27$–32) ions colliding with atoms. The fitting parameters, $P(nl)$, combined with the calculated transition probabilities are used for synthetic spectra. The best-fit parameters $P(nl)$ are given in Table II.

extending up to close to the ionization limit for each charge state ion, though they become progressively less intense. This suggests that, instead of direct transition from the captured Rydberg state to the $(2l)$ ground state, the indirect cascade transitions are dominant, as previously observed in collisions of ions with a single K-shell vacancy [3]. Their peak positions clearly move toward high energy as the ion charge increases from $q=27$ (a single L_3 shell electron ionized) to $q=33$ (all $2p$-shell and single $2s$-shell electrons ionized but only a single $2s$-shell electron left). The observed L x-ray spectra from the dominant transitions are compared with synthetic spectra which will be discussed in detail later. Only slight variations of L x-ray spectra have been observed when the target gas was changed.

B. L x-ray production cross sections

The observed L x-ray yields have been converted to absolute x-ray emission cross sections after normalizing to the known cross section for Ar K x-ray production in proton impact on Ar atoms, as mentioned above. The absolute cross sections have been determined only for Kr^{27+} ion impact on various target atoms and molecules. The results are shown in Fig. 2 and in Table I. Indeed total L x-ray production cross sections are found to increase roughly proportional to the inverse square of the ionization energy of target, either atom or molecule, as seen in Fig. 2. This trend is similar to that observed in K x-ray emissions from an ion with single K-shell vacancy [3].

This feature can be understood based upon the extended classical over-barrier model [12] in which total electron-capture cross sections closely relate with the ionization energy I_b of target. So far various empirical formulas already had been proposed to get/estimate total electron-capture cross sections [13,14]. This model has been known to successfully predict that total electron-capture cross sections are proportional to the ion charge (q) as well as to the inverse square of the ionization energy of target [13], given as follows:

$$\sigma_t = \frac{2.6q}{(I_b)^2} \quad (10^{-13}\mathrm{cm}^2), \tag{3.1}$$

where q is the charge of the primary ion and I_b the first ionization energy of target (in units of eV). This formula suggests that the electron-capture cross sections depend only on the ion charge but not on the electron-shell ionized. Therefore it should be noted that the cross sections are independent of the shells of the primary ions where the electrons are present. Indeed, this and a similar empirical formula [14] also had been confirmed to reproduce quite nicely the observed total electron-capture cross section data for rare-gas atoms and molecules over a wide range of parameters (q, I_b) independent of vacancy or ionized states present in the incident ions [15].

C. Comparison with electron-capture cross sections

In the present paper, as shown above, we have determined absolute L x-ray emission cross sections in collisions of Kr^{27+} ions with various neutral targets. Then, it is interesting to know what fraction of the electron-captured Kr^{26+} ions emit L x rays. The observed ratios of L x-ray emission cross sections, relative to total electron-capture cross sections estimated based upon an empirical formula [13], are summarized in the fourth column of Table I which shows that ratios are nearly independent of targets. It has been found that the average ratios over all the targets including molecules investigated in the present paper are roughly 0.4. This suggests that 60% of total electron-capture processes do not emit x rays within a limited viewing zone of the present detector, indicating that a large fraction of the electron-captured ions result in the metastable states with regard to x-ray emission.

In collisions involving Kr^{27+} ions where the final state after a series of cascading process resulting in L x-ray emission is only L_3 state, as schematically shown in Fig. 3, the corresponding transitions can be only $L\alpha_1$ (from M_5), $L\alpha_2$ (from M_4), $L\beta_{2,15}$ (from N_4,N_5), $L\beta_5$ (from $O_{4,5}$), $L\beta_6$ (from N_1), and Ll (from M_1) x rays [16]. Thus, transitions from other excited states such as M_2 and M_3 states are prohibited through the selection rule, indicating that the ion with an electron cascading down to these states cannot emit L x rays if the intrashell interactions or mixing are neglected. It is not easy to directly compare the observed ratios with the calculated ratios as they depend on a number of parameters such as transition probabilities as well as the initial $(n_0 l_0)$-state distributions just after electron-capture. It is necessary to develop models to understand the observed spectra in detail (see next section).

Furthermore, it is expected that intrashell interactions such as Coster-Kronig transition in the same n shell can play a significant role in changing the intermediate $(n_i l_i)$-state distributions through cascade and thus in determining the final $(n_f l_f)$-state distributions just before L x-ray emission which are indeed one of the key issues in shaping the final x-ray spectrum.

D. L x-ray spectrum synthesis

The observed L x-ray spectra and shapes are strongly dependent upon a number of parameters in electron-capture collision, cascade, and transition processes. Among them, the most important are

(a) The final electronic $(n_f l_f)$ distributions and

(b) The transition probabilities in the final $(n_f l_f)$ states.

The final electronic $(n_f l_f)$ distributions are determined by the following parameters:

(c) The initial $(n_0 l_0)$ distributions just after electron capture;

TABLE II. $P(n_f l_f)$ parameters used in synthetic L x-ray spectra from Kr^{q+} (q=27–33) ions colliding with atoms.

$n_f l_f$	Kr^{27+}	Kr^{28+}	Kr^{29+}	Kr^{30+}	Kr^{31+}	Kr^{32+}	Kr^{33+}
$3s$	1	1	1	1	1	1	1
$3d$	1/100	1/60	1/100	1/20	1/20	1/10	1/80
$4s$	1/50	1/10	1/5	1/5	1/5	1	1/5
$4d$	1/200	1/200	1/200	1/50	1/35	1/25	1/100
$3p$	0	0	0	4	5	5	1/30
$4p$	0	0	0	0	0	2	1/30

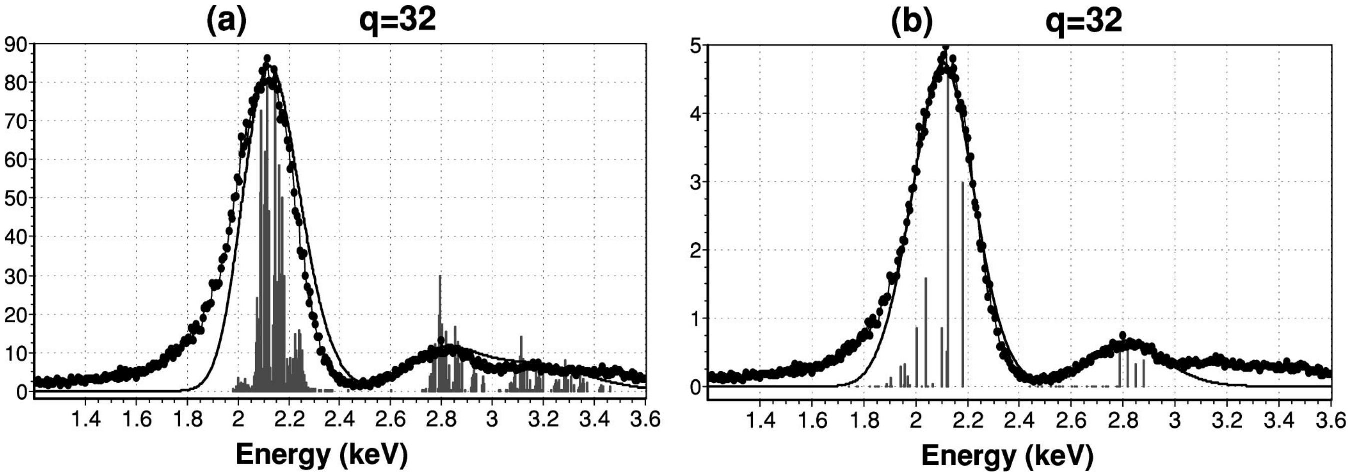

FIG. 6. Comparison between the observed and synthetic L x-ray spectra from Kr^{32+} ion colliding with Ne atoms. (a) Only the calculated transition probabilities with statistical populations. (b) The fitting parameters $P(nl)$ given in Table II are used.

(d) The transition probabilities and branching ratios of the intermediate (n_il_i) states during cascade processes;

(f) Intrashell interactions which may change the intermediate (n_il_i) distributions during cascade.

As mentioned above, the number of the initial (n_0l_0) states just after electron-capture at low energies is known to be distributed over a limited range. On the other hand, the number of cascades can be as large as ten which means that a huge number of the electronic states through cascade processes are involved before reaching the final x-ray emission stages and thus more than 1000 states have to be taken into account all the way down to the ground state.

So three relatively simple ways have been used to synthesize spectra in the present paper.

(1) The first one is simply to use the calculated transition probabilities for all the possible electronic states, assuming their statistical population distributions.

To create the synthetic x-ray spectrum, first we have calculated the transition energy (E_0^n) and the (weighted) transition intensity (g_nI_n) where g is defined as the statistical weight, covering all the possible (nth) transitions, using the Cowan code [18]. We calculate excitation energies and radiative transition rates for the $2s^22p^n$-$2s^22p^{n-1}3l$, and $2s2p$-$2s3l$ transitions with $l=s$, d and $n=6$-1 in Kr^{26+}-Kr^{32+}. We consider also all possible $2s2p^n-2s^22p^{n-2}3p$ transitions as well as $2s^22p^n$-$2s^22p^{n-1}4l$ and $2s^22p^n$-$2s^22p^{n-1}5l$ transitions with $l=s$, d and $n=6$-1 in Kr^{26+}-Kr^{32+}. Complete number of transitions included in our synthetic spectra presented in Fig. 4 is equal to 28 (Ne-like Kr), 245 (F-like Kr), 935 (O-like Kr), 1608 (N-like Kr), 1427 (C-like Kr), 628 (B-like Kr), and 269 (Be-like Kr).

It is assumed that the spectral (energy) distribution of each transition can be expressed with a Gaussian profile with the resolution of δE_n (which is mostly due to the detector resolution and here is assumed to be constant for a particular ion and is slightly varied over 5–10% for different charge ions to find the best fit to the observed spectrum). Summing up the Gaussian profiles for all the possible N transition lines composing the observed spectrum, the final synthetic spectrum can be expressed as a function of energy (E) in the following form:

$$I_S(E)=A\sum_{n=1}^{N} g_nI_n(E_0^n)2\sqrt{\frac{\ln 2}{\pi}}\frac{1}{\delta E_n}\times\exp\left[-4\ln2\left(\frac{E-E_0^n}{\delta E_n}\right)^2\right]. \tag{3.2}$$

Here the factor A is an adjustable parameter to get the best fit with the observed spectrum.

As expected, this technique cannot reproduce the observed x-ray spectra and indeed significant discrepancy between the synthetic and the observed spectra is seen for all the ions, as shown in Fig. 4. Obviously this discrepancy originates from negligence of the proper electronic state distributions just before x rays are emitted.

(2) The second technique to synthesize the spectra is to completely neglect the detailed transitions from the initial (n_0l_0) distributions in electron-capture through cascading processes but to simply try to reproduce the observed spectra by fitting the calculated spectra under assumption that the final (n_fl_f)-distribution parameter, $P(n_fl_f)$, is used as a fitting parameter. This parameter represents the final electronic state distributions when x rays are emitted. Then x-ray spectrum is determined by $P(n_fl_f)A_r(n_fl_f)$ where $A_r(n_fl_f)$ is the radiative transition probability of the (n_fl_f) state. In the present analysis, the summation is performed over those with relatively large transition probabilities. As shown in Fig. 5 with the best-fitted parameters $P(n_fl_f)$ given in Table II, the synthetic spectra seem to produce nicely the observed spectra for all the ions investigated in the present paper.

As noticed in Fig. 5, there are still some discrepancies at the lower-energy side. It is believed that this is caused by incomplete collection of electrons produced in x-ray collisions with the Si crystal [17]. It is important to note here that the distribution parameters best fitted to the observed spectra have changed only slightly when the ion charge increases from $q=27$ to 33. Indeed it has been found that the main contribution to the x-ray peaks in the synthetic spectra comes from the $3s$ states, with only a small contribution from other states, for all the ion charges, as shown in Fig. 5.

In Fig. 6, we present similar L x-ray spectra from $\sim$2-keV/uKr^{32+} ions in collisions with Ne atoms.

This suggests that the electron cascade to the final $3s$ states to emit L x rays may be more likely than to the $3p$ states in hydrogenic ions as the probabilities of $3s \rightarrow 2l$ transitions are generally smaller than those of $3p$-$2l$ transitions [19]. Another reason for this can be due to the fact that there is no $2s$ vacancy, except for Kr^{33+} ions. Thus, any transitions leading to the $2s$ state are not possible or the relevant states are metastable if no intrashell interactions are taken into account. Thus the contribution from $3p$ states to x-ray emission is strongly suppressed for all Kr^{q+} ions ($q \leqslant 32$). This may also explain why such significant fractions ($\sim$60%) of the electron-captured ions cannot emit the L x rays.

(3) Finally, a time-dependent collisional-radiative model that was originally developed to describe x-ray emission from hot, dense, laser-produced plasmas was modified to describe the emission processes in the present paper. Starting with initial populations X_i in states i, this model numerically propagates the radiative transfer of population to lower states using coupled rate equations:

$$\frac{dX_i}{dt} = \sum_{j>i} X_j A_r(j \rightarrow i) - X_i \sum_{j<i} A_r(i \rightarrow j). \tag{3.3}$$

The intensity of a transition is determined by the time-integrated population of its upper level and its radiative decay rate. The synthetic spectra are constructed as in the previous subsection 1.

The kinetic model includes all LS states of four ions with configurations $2s^2 2p^k$ and $2s^2 2p^{k-1} nl$, where k varies from six (Kr^{27+}) to 3 (Kr^{30+}) and n ranges from three to six. The energy-level structures of the ions and all $E1$ radiative decay rates were calculated with the Cowan code [18]. In addition, for Kr^{27+}, all $E2$, $M1$, and $M2$ radiative decay rates from excited states with $n<6$ to the ground state were calculated with second-order MBPT [20].

As noted above, the actual population distribution right after capture is concentrated in states with $n=9$–13, which are not modeled [see Eq. (1.1)]. However, most of the experimentally observed emission is from $n>5$, so the initial distribution will have only an indirect influence on the final spectrum as long as it is concentrated in states with $n>5$. Also, it has been shown that the distribution after capture in keV/u collisions is roughly statistical [21]. So the initial population is taken to be statistically distributed among the $n=6$ states, preserving these two important properties of the actual initial state.

The time-dependent populations of Kr^{27+} states are shown in Fig. 7. the x-ray emission in the spectral region of interest occurs when population moves from an excited state to the ground state. The bulk of x-ray emission occurs in less than 1 ns. The population at 1 ns is concentrated in the ground state and the metastable state $2s^2 2p^5 3s\,^3P_2$, which has a magnetic quadrupole decay rate of the order of $10^6\ \mathrm{s}^{-1}$. After 1 ns, only 56% of the captured electrons have undergone radiative decay to the ground state. This confirms the hypothesis that the low x-ray yield from Kr^{27+} collisions (see Sec. III C) is due mainly to the retention of captured electrons in metastable states. The average time-integrated populations of nl states with relatively large radiative decay rates are given in Table III for comparison with $P(n_f l_f)$ from Table II. The agreement is best for Kr^{27+} and worst for Kr^{29+}.

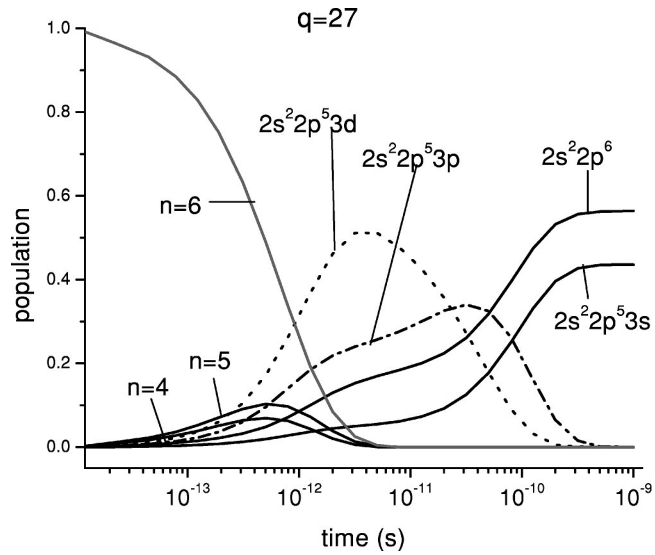

FIG. 7. Time-dependent population after electron-capture into $n=6$ of Kr^{27+}.

Comparisons between the experimental data and the synthetic spectra calculated with this model are given in Fig. 8. In all cases, the intensity of the contributions from $n=4$ and 5 fit the experimental data quite well. For the contributions from $n=3$, the shift of the main x-ray peak to lower energies is best for Kr^{27+}, which has the fewest states per excited configuration, and worst for Kr^{29+}, which has the most. Better fit for Kr^{29+} ion collisions is expected to be obtained by taking into account states with $n>6$.

IV. CONCLUDING REMARKS

We have observed L x-ray spectra for $\sim$2-keV/uKr^{q+} ($q=27$–33) ions colliding with various neutral atoms and molecules and also determined their absolute L x-ray emission cross sections for Kr^{27+} ions which have been found to be proportional to the inverse square of the target ionization energy, agreeing with the classical picture of electron-capture process. Then, these L x-ray production cross sections are

TABLE III. Average time-integrated populations of nl states with large A_r in the time-dependent kinetic model.

$n_f l_f$	Kr^{27+}	Kr^{28+}	Kr^{29+}	Kr^{30+}
$3s$	1	1	1	1
$3d$	1/96	1/17	1/8	1/3
$4s$	1/40	1/45	1/33	1/7
$4d$	1/220	1/130	1/62	1/26

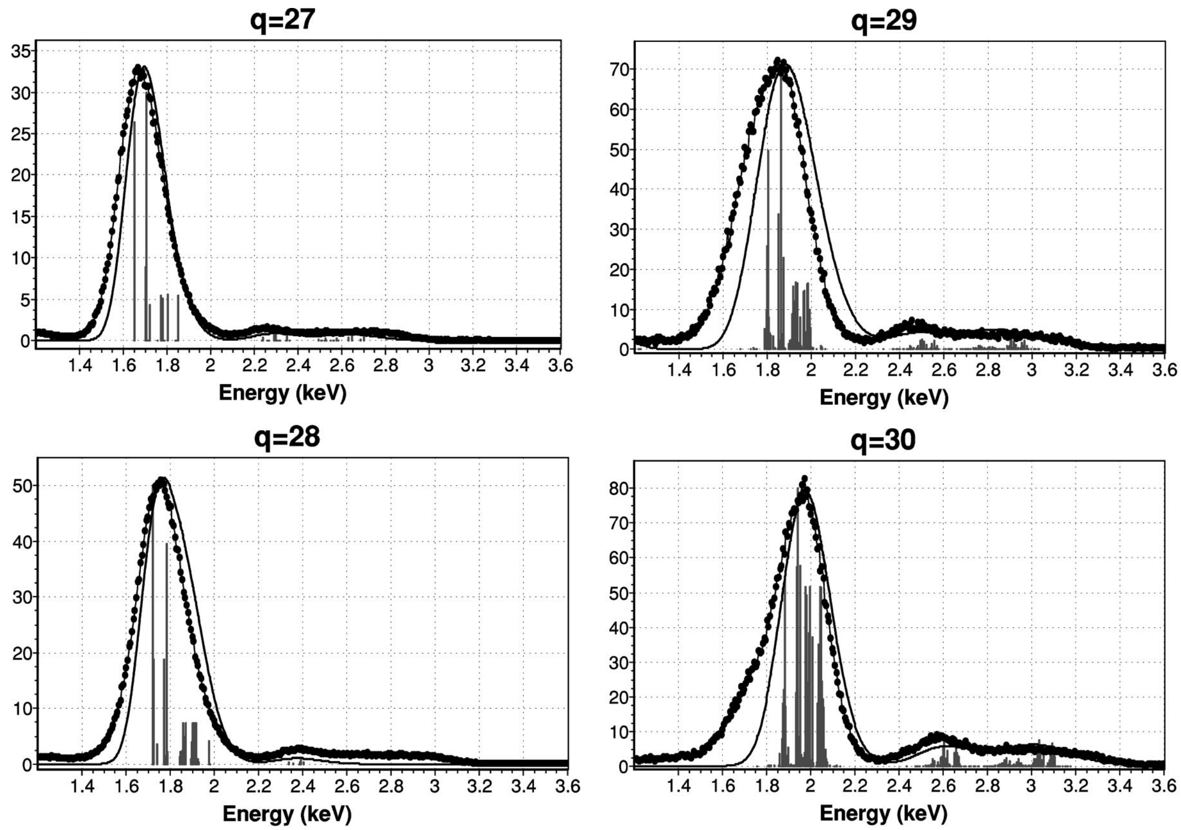

FIG. 8. Comparison between observed and synthetic x-ray spectra for Kr^{q+} ($q=27$–30) ions colliding with atoms. Line intensities of the synthetic spectra are proportional to radiative decay rates and time-integrated populations.

compared with total electron-capture cross sections based upon an empirical formula of Kimura *et al.* [13] and have been found that only roughly 40% of total electron-capture processes result in L x-ray emission and others in the metastable states without emitting x rays within the viewing zone of the detector.

We also have synthesized L x-ray spectra using different methods. Though so many transitions are involved in the electron-capture cascade processes, we have found a simple way to nicely reproduce the observed spectra, when the final electronic state distribution function is used as a fitting parameter, combined with the calculated transition energy and transition probability. This analysis suggests that most of the contribution to L x-ray emission comes from $3s\rightarrow 2p$ transitions. We have also discussed some common features with parameters used in plasma modeling code. It would be important to extend similar experiments to a higher charged Kr^{q+} ion ($q\geqslant 28$), which has more L-shell vacancies (in particular, Kr^{34+} ions where no L-shell electron is left anymore) and, thus, more different transitions can occur, in order to know variations of ratios of L x-ray emission cross sections over total electron-capture cross sections.

ACKNOWLEDGMENTS

The authors would like to thank C. Fehrenbach and Paul Gibson for providing the ion beam used in the present experiment and Rami Ali for helpful discussions. This work (H.T.) was supported in part by the Chemical Sciences, Geosciences and Biosciences Division, Office of Basic Energy Science, Office of Science, U.S. Department of Energy. U.I.S. acknowledges partial support by Grant No. B503968 from Lawrence Livermore National Laboratory.

[1] R.K. Janev and H.P. Winter, Phys. Rep. **117**, 265 (1985).
[2] C.M. Lisse, K. Dennerl, J. Englhauser, M. Hayden, F.E. Marshall, M.J. Mumma, R. Petre, P. Pye, M.J. Ricketts, J. Schmitt, J. Trümper, and R.G. West, Science **274**, 205 (1996).
[3] H. Tawara, P. Richard, U.I. Safronova, and P.C. Stancil, Phys. Rev. A **64**, 042712 (2001) and references therein.
[4] J.B. Greenwood, I.D. Williams, S.J. Smith, and A. Chutjian, Phys. Rev. A **63**, 062707 (2001).
[5] P. Beiersdorfer, R.E. Olson, G.V. Brown, H. Chen, C.L. Harris, P.A. Neill, L. Schweikhard, S.B. Utter, and K. Widmann, Phys. Rev. Lett. **85**, 5090 (2000).
[6] V.A. Boiko, A.V. Vinogradov, S.A. Pikuz, I. Yu. Skobeiev, and A. Yu. Faenov, J. Sov. Laser Res. **6**, 82 (1985).
[7] Y.-K. Kim, D.H. Baik, P. Indelicato, and J.P. Desclaux, Phys. Rev. A **44**, 148 (1991).
[8] R.E. Olson, Phys. Rev. A **24**, 1726 (1981).
[9] K.R. Cornelius, K. Wojitkowski, and R.E. Olson, J. Phys. B **33**, 20l7 (2000).

[10] N. Nakamura, F.J. Currell, A. Danjo, M. Kimura, A. Matsumoto, S. Ohtani, H.A. Sakaue, M. Sakurai, H. Tawara, H. Watanabe, I. Yamada, and M. Yoshino, J. Phys. B **28**, 2959 (1995).
[11] K.G. Harrison, H. Tawara, and F.J. de Heer, Physica (Amsterdam) **66**, 16 (1973).
[12] A. Niehaus, J. Phys. B **19**, 2925 (1986).
[13] M. Kimura, N. Nakamura, H. Watanabe, I. Yamada, A. Danjo, K. Hosaka, A. Matsumoto, S. Ohtani, H.A. Sakaue, M. Sakurai, H. Tawara, and M. Yoshino, J. Phys. B **28**, L643 (1995).
[14] N. Selberg, C. Biedermann, and H. Cederquist, Phys. Rev. A **54**, 4127 (1996).
[15] K. Hosaka, H. Tawara, I. Yamada, H.A. Sakaue, F. Krok, S. Ohtani, A. Danjo, H. Watanabe, M. Kimura, A. Matsumoto, M. Sakurai, and M. Yashino, Phys. Scr., T **73**, 273 (1997).
[16] S.I. Salem, S.I. Panossian, and R.A. Krause, At. Data Nucl. Data Tables **14**, 91 (1974).
[17] U. Lehnert, M.P. Stockli, and C.L. Cocke, J. Phys. B **31**, 5117 (1998).
[18] R. D. Cowan, *The Theory of Atomic Structure and Spectra* (University of California Press, Berkeley, 1981).
[19] I. I. Sobelman, *Atomic Spectra and Radiative Transitions* (Springer, New York, 1992), p. 281.
[20] U.I. Safronova, C. Namba, I. Murakami, W.R. Johnson, and M.S. Safronova, Phys. Rev. A **64**, 012507 (2001).
[21] J.A. Perez, R.E. Olson, and P. Beiersdorfer, J. Phys. B **34**, 3063 (2001).